

Lawrence Berkeley National Laboratory

Physics

Title

Extracting constraints from direct detection searches of supersymmetric dark matter in the light of null results from the LHC in the squark sector

Permalink

<https://escholarship.org/uc/item/413531qh>

Journal

Physical Review D, 93(3)

ISSN

2470-0010

Authors

Riffard, Q
Mayet, F
Bélanger, G
[et al.](#)

Publication Date

2016-02-01

DOI

10.1103/physrevd.93.035022

Peer reviewed

Extracting constraints from direct detection searches of supersymmetric dark matter in the light of null results from the LHC in the squark sector

Q. Riffard,¹ F. Mayet,^{1,*} G. Bélanger,² M.-H. Genest,¹ and D. Santos¹

¹*LPSC, Université Grenoble-Alpes, CNRS/IN2P3, 38026 Grenoble cedex, France*

²*LAPTH, Université Savoie Mont Blanc, CNRS, BP 110, 74941 Annecy-Le-Vieux, France*

(Dated: March 2, 2018)

The comparison of the results of direct detection of Dark Matter, obtained with various target nuclei, requires model-dependent, or even arbitrary, assumptions. Indeed, to draw conclusions either the spin-dependent (SD) or the spin-independent (SI) interaction has to be neglected. In the light of the null results from supersymmetry searches at the LHC, the squark sector is pushed to high masses. We show that for a squark sector at the TeV scale, the framework used to extract constraints from direct detection searches can be redefined as the number of free parameters is reduced. Moreover, the correlation observed between SI and SD proton cross sections constitutes a key issue for the development of the next generation of Dark Matter detectors.

PACS numbers: 95.35.+d, 14.80.Ly

Direct detection of Weakly Interacting Massive Particles (WIMP) faces a long-standing difficulty inherent in the use of various target nuclei. The comparison of experimental results must be done at the level of the WIMP-nucleon interaction, which requires model-dependent, or even arbitrary, assumptions. The elastic scattering of a WIMP on a nucleon receives contribution from both the spin-independent (SI) interaction and the spin-dependent (SD) one. Hence, for a given experimental result, one of the interactions has to be neglected in order to draw conclusions for the other. This is obviously an arbitrary choice when the natural isotopic composition of the target material contains a large fraction of odd- A nuclei, as it is the case for natural Xenon ($\sim 47\%$) or natural Fluorine ($\sim 100\%$). Further assumptions must be made as the WIMP scattering occurs either on proton or neutron. There is no particular reason to fix the ratio of the coupling constants to a given value or to neglect the contribution of one type of nucleon. In the SI sector, the standard procedure is to assume a unique isospin-conserving coupling constant. On the contrary, in the SD sector, the results are usually presented with the assumption that the WIMP couples exclusively to one type of nucleon, while such hypothesis is not supported by any theoretical model. The method proposed in [1] allows one to account for SD scattering on protons and neutrons but still requires to neglect SI interaction.

We focus on the recent search results at the LHC (*e.g.* [2]) setting lower limits on the mass of the first and second generation squarks which can be as high as 1.8 TeV, depending on the models and parameter values. These limits could be quickly pushed even further if the squarks are not seen in the first Run 2 data. If these squarks are at the TeV level, we show in this Paper that the framework used to present the results of direct detection searches may be simpli-

fied. In particular, no arbitrary assumptions are needed as SI and SD interactions can be both taken into account.

First, in section I we recall for the reader's convenience the basic relations concerning direct detection that are used in the standard framework, presented in section II, to compare the results of direct detection searches. In section III, the SD and SI coupling ratios are evaluated within the framework of supersymmetry. The latest squark results at the LHC are then presented in section IV. We check in section V the implication for direct detection thanks to a scan of the supersymmetric parameter space. Finally, we present in section VI a new framework to extract constraints from direct detection searches

I. THEORETICAL CONTEXT

Direct detection is based on the elastic scattering of a WIMP on a target nucleus ${}^A\text{X}$ of mass m giving an observed recoil energy E_r . The rate is given by

$$\frac{dR}{dE_r} = \frac{\rho_0}{2m_\chi\mu^2} [\sigma^{\text{SI}} F_{\text{SI}}^2 + \sigma_0^{\text{SD}} F_{\text{SD}}^2] \mathcal{I} \quad (1)$$

with m_χ the WIMP mass, ρ_0 the local WIMP density and μ the WIMP-nucleus reduced mass. The \mathcal{I} term is given by

$$\mathcal{I} = \int_{v_{\min}} \frac{f(\vec{v})}{v} d^3v \quad (2)$$

where $f(\vec{v})$ is the WIMP velocity distribution and $v_{\min} = \sqrt{E_r m / 2\mu^2}$ is the minimal WIMP velocity required to produce a recoil of energy E_r . The WIMP-nucleus cross section at zero momentum transfer is obtained [3] by adding coherently the spin-dependent (SD) WIMP-nucleus cross section (σ^{SD}) and the spin-independent (SI) WIMP-nucleus cross section (σ^{SI}), weighted by the form factors (F_{SI} and F_{SD}) to account for the loss of coherence at large momentum transfer.

*Electronic address: mayet@lpsc.in2p3.fr

The SI WIMP-nucleus cross section is given by [4]

$$\sigma^{\text{SI}}(\frac{A}{Z}\text{X}) = \frac{4\mu^2}{\pi} (Zf_p + (A-Z)f_n)^2 \quad (3)$$

where $f_{p,n}$ is the WIMP-proton (resp. neutron) SI coupling constant.

The SD WIMP-nucleus cross section is given by [4]

$$\sigma^{\text{SD}}(\frac{A}{Z}\text{X}) = \frac{32}{\pi} G_F^2 \mu^2 \frac{J+1}{J} [a_p \langle S_p \rangle + a_n \langle S_n \rangle]^2, \quad (4)$$

where G_F is the Fermi constant, J the angular momentum of the target nucleus, $a_{p,n}$ the WIMP-proton (resp. -neutron) SD coupling constant, and $\langle S_{p,n} \rangle$ the spin content of the target nucleus. Note that the SD cross section may also be expressed in terms of the isoscalar and isovector combinations. As shown in [5], with proper normalization it is equivalent to Eq. 4.

We highlight the fact that in Eqs. 3 and 4, the relative sign of the WIMP-nucleon coupling constants may be such that constructive or destructive interferences may appear.

We introduce the SI and SD coupling ratios as:

$$C_f = f_p/f_n, \quad C_a = a_p/a_n \quad (5)$$

As discussed above C_f and C_a may be either positive or negative depending on the relative sign of the WIMP-nucleon coupling constants.

The SI and SD WIMP-nucleus cross sections are then given by

$$\sigma^{\text{SI}} = \frac{\mu^2}{\mu_p^2} \left(Z + \frac{(A-Z)}{C_f} \right)^2 \sigma_p^{\text{SI}} \quad (6)$$

and

$$\sigma^{\text{SD}} = \frac{\mu^2}{\mu_p^2} \frac{4}{3} \frac{J+1}{J} \left[\langle S_p \rangle + \frac{\langle S_n \rangle}{C_a} \right]^2 \sigma_p^{\text{SD}} \quad (7)$$

where μ_p is the WIMP-proton reduced mass and $\sigma_p^{\text{SI,SD}}$ the WIMP-proton cross sections.

II. STANDARD FRAMEWORK

The WIMP-nucleon interaction is thus described by 5 parameters ($m_\chi, \sigma_p^{\text{SD}}, C_a, \sigma_p^{\text{SI}}, C_f$), noticing that for a direct detector to be sensitive to SD interaction, the target nucleus must have a non-vanishing spin, whereas SI interaction is present for all nuclei.

For a given experimental result, the standard procedure is as follows. First, one has to neglect one of the interaction (SI or SD) in order to draw conclusions for the other (SD or SI). This may be referred to as a pure-SD (resp. -SI) case. Even then, further assumptions must be made as the nucleon content ($Z, N, \langle S_p \rangle$ and $\langle S_n \rangle$) depends on the target nucleus.

In the SI sector, the standard procedure is to consider that the SI coupling with proton and neutron are equal ($C_f = 1$). Isospin violation, leading to a cancellation of the proton and neutron contributions in some nuclei, has been proposed as an explanation of the discrepancy between the signals claimed by certain experiments which contradict exclusions set with xenon-based detectors [6–9].

In the SD sector, the standard procedure requires one to assume that the interaction on one type of nucleon dominates and the SD results are then presented in two independent planes: the pure-proton case ($a_n = 0$) and the pure-neutron one ($a_p = 0$). However, only the extreme nuclear shell model does predict that the spin of the nucleus is determined solely by the unpaired nucleon. Such an approximation leads to the wrong conclusion that, amongst odd-A nuclei, odd-Z (resp. odd-N) ones are sensitive to proton only (resp. neutron). In practice, the spin of the target nucleus is carried by both neutrons and protons [10] and the relative sign of $\langle S_{p,n} \rangle$ induces either constructive or destructive interferences, depending on the sign of the SD coupling ratio C_a , see *e.g.* [11]. Note that while the interferences are ignored in the current framework used to compare experimental results of direct searches obtained with various targets, they are taken into account in the numerical evaluations of the SD cross section, for instance in Micromegas [5] or DarkSUSY [12].

III. EXPECTED COUPLING RATIOS IN MSSM

In supersymmetry, two diagrams contribute at tree level to the SI interaction: the squark exchange in the s-channel and the Higgs boson exchange in the t-channel. For the light Higgs h , the SI coupling ratio is given by

$$C_f = \frac{m_p \sum_q g_{hq} f_{Tq}^p / m_q}{m_n \sum_q g_{hq} f_{Tq}^n / m_q} \quad (8)$$

where the summation is on all quarks including heavy ones, g_{hq} is the Higgs-quark-quark coupling constant and $f_{Tq}^{p,n}$ is related to the contribution of the quark q to the nucleon mass m_N . The values of $f_{Tq}^{p,n}$ are from [13] for light quarks (u, d, s) and from [14] for heavy ones (b, c, t). For a standard Yukawa coupling ($g_{hq} \propto m_q$), one finds that the SI coupling ratio is given by $C_f \simeq 0.985$. Note that in MSSM the second Higgs is heavy enough that its contribution is suppressed. We recall that the standard procedure is to consider only the value $C_f = 1$, thus ignoring the contribution of u and d quarks.

Two diagrams contribute to the SD interaction: the squark exchange in the s-channel and the Z boson exchange in the t-channel. For the latter, the coupling ratio C_a is given by

$$C_a = \frac{\Delta_u^p - \Delta_d^p - \Delta_s^p}{\Delta_u^n - \Delta_d^n - \Delta_s^n} \quad (9)$$

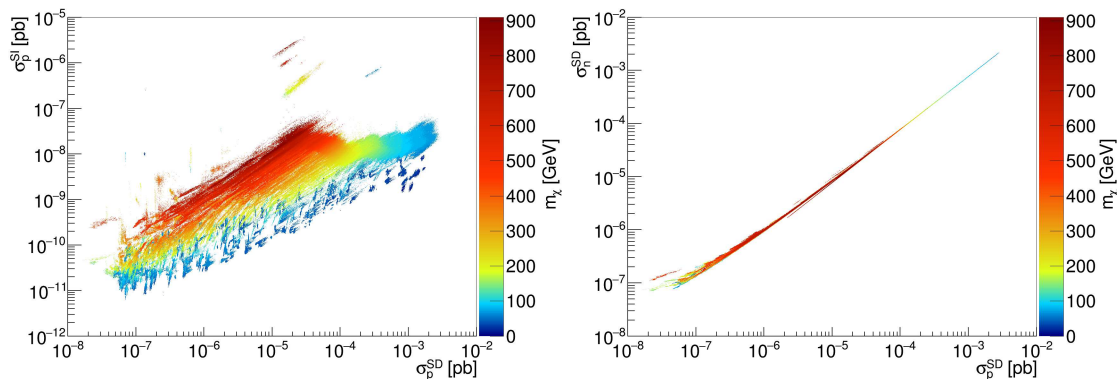


FIG. 1: Scan of the MSSM parameter space in the $(\sigma_p^{SD}, \sigma_n^{SD})$ plane (right) and in the $(\sigma_p^{SD}, \sigma_p^{SI})$ one (left). The mass of the first and second generation squarks has been fixed at a common value at 1.5 TeV. The color code indicates the WIMP mass.

where the coefficients Δ_q^N describe the contribution of a quark q to the spin of the nucleon. Using the values given in [15], the coupling ratio gets a model-independent value, $C_a = -1.14$, corresponding to a cross section ratio $\sigma_p^{SD}/\sigma_n^{SD} = 1.3$. The squark exchange contribution gives a value of C_a that depends on the exchanged squark [16]: $C_a = 1$ if the squark \tilde{q}_L contribution dominates and $C_a = -3.38$ for \tilde{q}_R . Note that a cancellation between the squark and Z exchange may lead to any value for C_a .

For heavy squarks, typically above ~ 500 GeV, the squark diagram is suppressed and the SD (resp. SI) interaction proceeds, at tree level, only via an exchange of Z (resp. Higgs) boson in the t-channel. Hence, the SD interaction is described by two coupling constants: g_{qqZ} , which only depends on standard model parameters and $g_{\chi\chi Z}$, which does not depend on the quark flavor. Same conclusion applies to the SI interaction, with $g_{\chi\chi h}$ and g_{qqh} .

The conclusion is twofold. First, when considering heavy squarks, the coupling ratios, C_f and C_a , become constant and independent of the supersymmetric parameters. As shown above, the values of C_f and C_a may be analytically evaluated. Second, SI and SD cross sections are expected to be correlated as the interaction is dominated by the strength of the coupling of quarks to Z and Higgs bosons (g_{qqh} and g_{qqZ}).

IV. HEAVY SQUARKS AT THE LHC

At the LHC, squarks could be produced in strong interaction processes and cascade decay to the stable lightest sparticle, leading to final states containing jets, missing transverse momentum and possibly leptons.

The inclusive searches for the first and second generation squarks performed by ATLAS during the Run 1 of the LHC have been summarized in [2]; limits were placed in a variety of models. For given SUSY breaking models within the framework of the Minimal Supersymmetric Standard Model (MSSM), such as the

mSUGRA/CMSSM [17] or the NUHMG [18] models considered in [2], squark masses up to around 1.6 TeV and 900 GeV are excluded, respectively. Results on simplified models are also reported; these models are based on an effective Lagrangian considering only one specific production and decay chain, with all other sparticles decoupled. The limits in these models depend on the decay chain assumed. For a direct decay $\tilde{q} \rightarrow q\tilde{\chi}_1^0$ (with an eightfold squark mass degeneracy), $m_{\tilde{q}} < 850$ GeV is excluded for $m_{\tilde{\chi}_1^0} < 100$ GeV. For very compressed scenarios, the limit is less stringent, at around 440 GeV. If the squark decays instead via an intermediate chargino, $m_{\tilde{q}} < 790$ GeV is excluded for $m_{\tilde{\chi}_1^0} < 100$ GeV. For longer decay chains, the exclusion is weaker in the compressed region. If the squark decays via a chargino or neutralino and a slepton, $m_{\tilde{q}} < 820$ GeV is excluded for $m_{\tilde{\chi}_1^0} < 100$ GeV.

A more general study can be performed by scanning the 19-parameter space of the p(henomenological)MSSM, the most general version of the R-parity conserving MSSM obtained after applying experimentally driven constraints. Such a scan was performed in [19] to assess the coverage of the ATLAS and CMS SUSY searches. The scan shows that the first and second generation squarks can have lower masses than the limits described above, especially at large gluino masses, as the pMSSM spectrum can be more complex than the assumed SUSY breaking scenarios or simplified models. However, the scan still excludes most models with $m_{\tilde{q}} < \mathcal{O}(500)$ GeV. A similar scan was performed by the ATLAS Collaboration [20]; no models with a first or second generation squark of mass $m_{\tilde{q}} < 250$ GeV survive the exclusion set and a majority of the models with $m_{\tilde{q}} < 450$ GeV is excluded. A projection study for the LHC is also performed in [19]; if nothing is found, most models with squark masses below $\mathcal{O}(1 - 1.5)$ TeV should be excluded with 300 fb^{-1} of data at 14 TeV.

Constraint	Value	Sys./Stat./Th. error	Ref.
$\Omega_{\text{CDM}}h^2$	0.1187	0.0017/ - /0.0119 (10%)	[21]
m_h, μ_{VBF} and $\Delta\Gamma h$	combined analysis (HiggsSignals)	-	[22–24]
$a_\mu^{\text{exp}} - a_\mu^{\text{SM}}$	26.1×10^{-10}	$(8.0/ - /10.0) \times 10^{-10}$	[25]
$\Delta\rho$	≤ 0.002	-	[26]
$\tan\beta(m_A)$	Fig. 3 in [27]	-	[27]
$\mathcal{BR}(B_s^0 \rightarrow \mu^+ \mu^-)$	2.9×10^{-9}	$(0.7/ - /0.29) \times 10^{-9}$	[28]
$\mathcal{BR}(b \rightarrow s\gamma)$	3.43×10^{-4}	$(0.07/0.21/0.23) \times 10^{-4}$	[29]
$\mathcal{BR}(B^+ \rightarrow \tau\nu_\tau)$	1.63×10^{-4}	$(0.54/ - /-) \times 10^{-4}$	[26]
$\mathcal{BR}(e^+e^- \rightarrow q\bar{q}\tilde{\chi}_1^0)$ @208GeV	≤ 0.05 pb	-	[30]
$\Delta\Gamma_Z$	< 2 MeV	-	[31]

TABLE I: Experimental constraints used for the likelihood function. For each parameter we present the experimental value together with the systematic (Sys.), statistic (Stat.) and theoretical (Th.) errors.

Parameter	Min.	Max.	Tol.	Parameter	Min.	Max.	Tol.
M1	1	1000	3	M_A	50	2000	4
M2	100	2000	30	$A_t = A_b$	-5000	5000	100
M3	1000	5000	8	A_l	-3000	3000	15
μ	50	1000	0.1	$M_{\tilde{t}_R}, M_{\tilde{t}_L}$	70	2000	15
$\tan\beta$	1	55	0.01	$M_{\tilde{q}_3}$	300	2000	14
$M_{\tilde{u}_3} = M_{\tilde{d}_3}$	300	2000	14	$M_{\tilde{q}_1} = M_{\tilde{q}_2} = 1.5$ TeV			

TABLE II: Intervals of free parameters used for the MSSM scan (in GeV). For each parameter we present the minimum and maximum values (Min. and Max.) and the step of the sampling (Tol.).

V. SCANNING THE MSSM PARAMETER SPACE

In order to assess the consequences of heavy squarks for the direct detection of dark matter, the MSSM parameter space has been scanned, following [32], via a Markov Chain Monte Carlo method, based on micrOMEGAs3.6 [13] and SuSpect [33]. The intervals of the free parameters are presented in Tab. II. Note that we impose a common mass for the first and second generation squarks at 1.5 TeV, while third generation squarks can have masses between 300 GeV and 2 TeV. The likelihood function gets contributions from Dark Matter relic density [34], Higgs mass and invisible width [35], collider constraints on rare branching ratios and MSSM parameters [36] and $a_\mu = (g-2)_\mu/2$ [25], see Tab. I. No constraints from direct detection are applied. Note that the relic density sets a strong constraint on the SUSY parameter space. By doing so, we choose to impose the Planck constraint and limit the results to standard thermal relic. However, it does not affect the applicability of the method proposed in Sec. VI as it is only based on the squark mass limit.

Figure 1 (right) presents the $(\sigma_p^{SD}, \sigma_n^{SD})$ plane for all MSSM models compatible with cosmology and collider physics, for 1.5 TeV squark mass. It can be seen that for all WIMP masses, the SD cross section on proton and neutron are highly correlated. Note that we also checked that the SI cross sections on proton and neutron are also highly correlated, as expected. The left panel presents

the same models in the $(\sigma_p^{SD}, \sigma_p^{SI})$ plane. A correlation between SI and SD cross sections is observed at all WIMP masses. For a given value of the SI cross section, the values of the SD one span about two orders of magnitude. Hence, the correlations expected in the case of heavy squarks are assessed in generic MSSM models constrained by current collider and cosmology results.

VI. A NEW FRAMEWORK TO PRESENT CONSTRAINTS FROM DIRECT DETECTION SEARCHES

Within this framework, the number of free parameters is thus reduced to three ($m_\chi, \sigma_p^{SD}, \sigma_p^{SI}$) as the coupling ratios get constant values, $C_a = -1.14$ and $C_f = 0.985$. This allows us to redefine the procedure used to compare the results of direct detection searches.

For the sake of completeness, we consider a detector composed of several target nuclei with fraction g_i . The measured rate R_{mes} reads:

$$R_{mes} = \frac{\rho_0}{2m_\chi} \sum_i \frac{g_i}{\mu_i^2} \int_{\Delta E} \frac{dR_i}{dE_r} \mathcal{A} dE_r \quad (10)$$

where the integral is performed over the energy window ΔE and $\mathcal{A}(E_r)$ is the acceptance function. Using eq. 1, 6 and 7, the measured rate reads

$$R_{mes} = \frac{\rho_0}{4\mu_p^2} \sigma_p^{SI} \sum_i g_i \left(Z_i + \frac{(A_i - Z_i)}{C_f} \right)^2 \mathcal{F}_i^{SI} + \sigma_p^{SD} \sum_i g_i \frac{4}{3} \frac{J_i + 1}{J_i} \left[\langle S_p \rangle_i + \frac{\langle S_n \rangle_i}{C_a} \right]^2 \mathcal{F}_i^{SD} \quad (11)$$

The \mathcal{F} parameters encode the whole energy dependence:

$$\mathcal{F}_i^{SD,SI} = \frac{2}{m_\chi} \int_{\Delta E} F_{\text{SD,SI},i}^2 \mathcal{A} \mathcal{I}_i dE_r \quad (12)$$

Hence for a given value of R_{mes} , the SD and SI WIMP-proton cross section are linked by a linear function:

$$\sigma_p^{SI} = b - a \times \sigma_p^{SD} \quad (13)$$

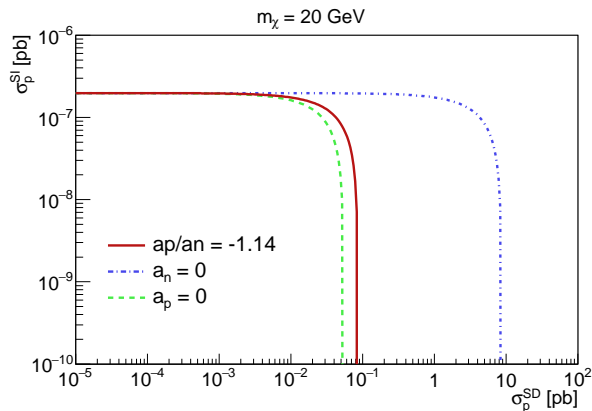


FIG. 2: Constraint in the $(\sigma_p^{SI}, \sigma_p^{SD})$ at $m_\chi = 20$ GeV from the result of [37]. The solid curve presents the result for $C_f = 0.985$ and $C_a = -1.14$, while the dashed (resp. dash-dotted) presents the pure-neutron (resp. proton) case.

with

$$a = \frac{4}{3} \times \frac{\sum_i g_i \frac{J_i+1}{J_i} \left(\langle S_p \rangle_i + \frac{\langle S_n \rangle_i}{C_a} \right)^2 \mathcal{F}_i^{SD}}{\sum_i g_i \left(Z_i + \frac{A_i - Z_i}{C_f} \right)^2 \mathcal{F}_i^{SI}} \quad (14)$$

and

$$b = \frac{\frac{4\mu_p^2}{\rho_0} R_{mes}}{\sum_i g_i \left(Z_i + \frac{A_i - Z_i}{C_f} \right)^2 \mathcal{F}_i^{SI}} \quad (15)$$

Note that a only depends on the detector properties, WIMP mass and halo model (Z), while b depends also on the measured rate R_{mes} . As discussed above, a squarks sector at the TeV scale implies that the coupling ratios get fixed values, $C_a = -1.14$ and $C_f = 0.985$. Hence, we propose to present the results of direct detection experiments in the plane $(\sigma_p^{SI}, \sigma_p^{SD})$ for a given value of m_χ . This enables a direct comparison of all experiments without any arbitrary assumptions, such as neglecting one type of interaction (either SI or SD).

For concreteness, we exemplify by presenting on Fig. 2 the result of one dark matter experiment, namely CDMS-II [37], in the $(\sigma_p^{SI}, \sigma_p^{SD})$ at $m_\chi = 20$ GeV. While the asymptotic values correspond to the standard procedure, pure-SI and pure-SD cases, the upper right-hand side of the curve corresponds to the case when both SI and SD interactions contribute to the event rate. This region was thus ignored in the standard procedure, unless when fixing the coupling ratios to arbitrary values, *e.g.* [38]. For SD interaction, we also present the pure-neutron and pure-proton cases. We note that our interpretation of this experimental result is slightly less constraining than in the pure-neutron case, due to destructive interferences between proton and neutron SD interaction induced by the relative sign of the spin contents of ^{73}Ge [39].

Figure 3 presents recent experimental results in the $(\sigma_p^{SI}, \sigma_p^{SD})$ and a comparison with the prediction of MSSM models. As all results presented within this new framework, the WIMP mass has to be fixed, $m_\chi = 100 \pm 10$ GeV in this case, which explains the thickness observed on experimental curves. For a given detector, when the SD limit has not been published, it has been calculated from SI result, using (13) and (15). It can first be noticed that this framework enables a direct comparison of the results of direct detection searches in all cases, even if only a fraction of the target material is composed of nuclei with a non-vanishing spin. Second, the usual distinction, *e.g.* [40], between detectors mainly sensitive to the SD interaction on proton (resp. neutron) is no longer relevant within this framework. Eventually, the strong correlation between SD and SI interaction must be emphasized. As stated above, the suppression of the squark s-channel in the context of heavy squarks explains this feature. This implies that the exclusion of MSSM models driven by pure-SI interaction ($\sim 10^{-9}$ pb on Fig. 3) applies to the SD sector an order of magnitude below the pure-SD case ($\sim 3 \times 10^{-5}$ pb).

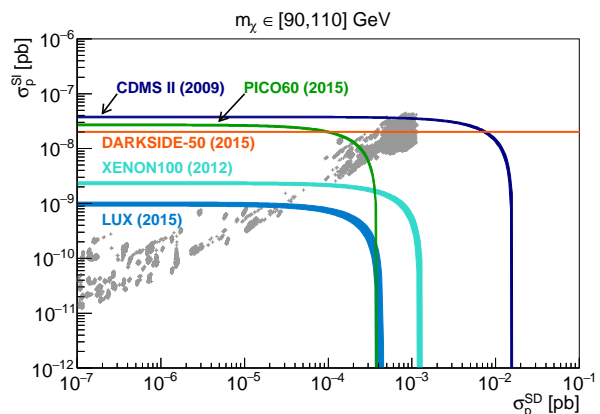


FIG. 3: Experimental constraints in the $(\sigma_p^{SI}, \sigma_p^{SD})$ for $m_\chi = 100 \pm 10$ GeV/ c^2 compared with the prediction of MSSM models. Data are extracted from [37, 41–45]. Note that the limit of CDMS has been improved by a factor ~ 2.4 [46] with respect to [37].

VII. CONCLUSION

The searches at the LHC are pushing the limits on the squark mass to higher values. We have shown that a heavy squark sector opens the possibility to redraw the landscape of direct detection of supersymmetric dark matter as the free parameter space is reduced from 5 parameters to only 3: the WIMP mass, the SD and SI proton cross sections. Within the context of supersymmetry, this new framework allows for a direct comparison of results of direct detection obtained from various target nuclei. No other assumption than the squark TeV mass

scale is needed. This framework also applies to other theories of dark matter for which the interaction takes place predominantly via the Z and Higgs exchange. Moreover, the strong correlation between SI and SD proton cross section, observed at all WIMP masses, is a key issue for the development of the next generation of Dark Matter detectors.

Acknowledgements

GB and MHG acknowledge partial support by the French ANR, Project DMAstro-LHC, ANR-12-BS05-0006.

-
- [1] D. R. Tovey, R. J. Gaitskell, P. Gondolo, Y. A. Ramachers and L. Roszkowski, *Phys. Lett. B* **488** (2000) 17
- [2] ATLAS Collaboration, *JHEP* **1510** (2015) 054
- [3] M. W. Goodman and E. Witten, *Phys. Rev. D* **31** (1985) 3059
- [4] J. Engel, S. Pittel and P. Vogel, *Int. J. Mod. Phys. E* **1** (1992) 1.
- [5] G. Belanger, F. Boudjema, A. Pukhov and A. Semenov, *Comput. Phys. Commun.* **180** (2009) 747
- [6] S. Chang *et al.*, *JCAP* **1008** (2010) 018
- [7] J. L. Feng *et al.*, *Phys. Lett. B* **703** (2011) 124
- [8] M. T. Frandsen *et al.*, *JCAP* **1307** (2013) 023
- [9] G. Bélanger *et al.*, *JCAP* **1402** (2014) 020
- [10] V. A. Bednyakov and F. Simkovic, *Phys. Part. Nucl.* **36** (2005) 131 [*Fiz. Elem. Chast. Atom. Yadra* **36** (2005) 257]
- [11] E. Moulin, F. Mayet and D. Santos, *Phys. Lett. B* **614** (2005) 143
- [12] P. Gondolo, J. Edsjo, P. Ullio, L. Bergstrom, M. Schelke and E. A. Baltz, *JCAP* **0407** (2004) 008
- [13] G. Bélanger *et al.*, *Comput. Phys. Commun.* **185** (2014) 960
- [14] M. A. Shifman, A. I. Vainshtein and V. I. Zakharov, *Phys. Lett. B* **78** (1978) 443
- [15] G. Jungman, M. Kamionkowski and K. Griest, *Phys. Rept.* **267** (1996) 195
- [16] G. Bélanger, E. Nezri, A. Pukhov, *Phys. Rev. D* **79** (2009) 015008
- [17] With parameters $\tan\beta=30$, $A_0 = -2m_0$ and $\mu > 0$.
- [18] Non-universal Higgs mass model with gaugino mediation with parameters $m_0 = 0$, $\tan\beta=10$, $\mu > 0$ and $m_{H_2}^2=0$.
- [19] M. Cahill-Rowley *et al.*, *Phys. Rev. D* **91** (2015) 055002
- [20] ATLAS Collaboration, *JHEP* **1510** (2015) 134
- [21] P. A. R. Ade *et al.* [Planck Collaboration], *Astron. Astrophys.* **571** (2014) A16
- [22] S. Chatrchyan *et al.* [CMS Collaboration], *Phys. Rev. D* **89** (2014) 9, 092007
- [23] G. Belanger, B. Dumont, U. Ellwanger, J. F. Gunion and S. Kraml, *Phys. Rev. D* **88** (2013) 075008
- [24] P. Bechtle, S. Heinemeyer, O. Stal, T. Stefaniak and G. Weiglein, *Eur. Phys. J. C* **75** (2015) 9, 421
- [25] K. Hagiwara *et al.*, *J. Phys. G* **38** (2011) 085003
- [26] K. Nakamura *et al.*, *J. Phys. G* **37** (2010) 075021.
- [27] CMS Collaboration, CMS-PAS-HIG-12-050
- [28] CMS and LHCb Collaborations, CMS-PAS-BPH-13-007, CERN-LHCb-CONF-2013-012,
- [29] Y. Amhis *et al.*, arXiv:1412.7515 [hep-ex].
- [30] G. Abbiendi *et al.*, *Eur. Phys. J. C* **35** (2004) 1
- [31] D. Abbaneo *et al.*, SLAC-REPRINT-2000-098.
- [32] D. Albornoz Vasquez *et al.*, *Phys. Rev. D* **82** (2010) 115027
- [33] A. Djouadi, J. -L. Kneur, G. Moultaka, *Comput. Phys. Commun.* **176**, 426-455 (2007)
- [34] P. A. R. Ade *et al.*, arXiv:1502.01589 [astro-ph.CO]
- [35] G. Bélanger *et al.*, *JHEP* **1302** (2013) 053
- [36] V. Khachatryan *et al.*, *JHEP* **1410** (2014) 160
- [37] Z. Ahmed *et al.*, *Science* **327** (2010) 1619
- [38] C. Marcos, M. Peiro and S. Robles, arXiv:1507.08625 [hep-ph].
- [39] V. Dimitrov, J. Engel and S. Pittel, *Phys. Rev. D* **51** (1995) 291
- [40] F. Ruppin *et al.*, *Phys. Rev. D* **90** (2014) 8, 083510
- [41] C. Amole *et al.*, arXiv:1510.07754.
- [42] P. Agnes *et al.*, arXiv:1510.00702
- [43] E. Aprile *et al.*, *Phys. Rev. Lett.* **109** (2012) 181301
- [44] E. Aprile *et al.*, *Phys. Rev. Lett.* **111** (2013) 2, 021301
- [45] D. S. Akerib *et al.*, arXiv:1512.03506
- [46] R. Agnese *et al.*, *Phys. Rev. D* **92** (2015) 7, 072003